



TIME-DELAYED PERONA-MALIK TYPE PROBLEMS

H. AMANN

ABSTRACT. We propose time regularizations for ill posed evolution equations of the type of the Perona-Malik equation of image processing, prove that they are well posed, and give numerical evidence for their superiority to the widely used space regularizations.

1. INTRODUCTION

Nonlinear diffusion filters are used in image processing to simultaneously smoothen noisy pictures and enhance sharp contrasts in brightness, This approach was initiated by the pioneering work of P. Perona and J. Malik [23]. These authors proposed a scale space technique based on the evolution problem

$$(1.1) \quad \begin{cases} \partial_t u - \nabla \cdot (g(|\nabla u|^2) \nabla u) = 0 & \text{on } \Omega \times (0, \infty), \\ u(\cdot, 0) = u^0 & \text{on } \Omega, \end{cases}$$

which has to be complemented by boundary conditions, no-flux conditions being the most appropriate choice. Here u^0 is the grey level distribution of a given (distorted) picture occupying a bounded domain Ω in \mathbb{R}^n (with $n \leq 3$ in most applications) and boundary Γ . For increasing values of t the functions $u(\cdot, t)$ are interpreted as successively restored and coarsened versions of u^0 . The diffusion coefficient $g(|\nabla u|^2)$ is designed to be very small near

Received November 12, 2005.

2000 *Mathematics Subject Classification.* Primary 68U10; Secondary 35K55, 35K90.

Key words and phrases. Image processing, regularization of backward parabolic problems.



‘edge points’, that is, points at which the spacial gradient ∇u is large, whereas it is relatively big at points in whose neighborhood u varies only slightly. Thus it is to be expected that small disturbances, represented by small values of $|\nabla u|$, are smoothed out since in the vicinity of such a point (1.1) is essentially a heat equation with strong smoothing effects. On the other hand, $g(|\nabla u|^2)$ is almost zero near edge points so that the diffusion flux is practically stopped and sharp edges are preserved. Typical examples for an ‘edge stopping function’ g , which, in fact, have been used by Perona and Malik, are

$$(1.2) \quad g(s) = 1/(1+s), \quad g(s) = e^{-s}, \quad s \geq 0.$$

Parameter dependent versions defined by $g_\lambda(s) := g(s/\lambda)$ are also employed, $\lambda > 0$ being a measure for the steepness of an edge to be preserved. Striking numerical experiments show (visually) that the desired effect is obtained: for small positive t the function $u(\cdot, t)$ is a sharper image than u^0 , and sharp edges are preserved rather well for large t .

Unfortunately, with the choice (1.2) for the edge stopping function, the Perona-Malik problem (1.1) is ill posed, in general. To see this, suppose that $S := S(t)$ is a regular level set of an appropriately smooth solution $u(\cdot, t)$ at some time instant $t \geq 0$. Then, near S ,

$$(1.3) \quad \begin{aligned} \nabla \cdot (g(|\nabla u|^2)\nabla u) &= g(|\nabla u|^2)\Delta u + 2g'(|\nabla u|^2)D^2u\nabla u \cdot \nabla u \\ &= g(|\nabla u|^2)\Delta_S u + h(|\nabla u|^2)\partial_\xi^2 u, \end{aligned}$$

where D^2u is the Hessian of u , Δ_S is the Laplace-Beltrami operator of S , the vector field $\xi := -\nabla u/|\nabla u|$ gives the direction of steepest descent of u , and

$$(1.4) \quad h(s) := g(s) + 2sg'(s), \quad s \geq 0.$$

Note that $h(0) = 1$ and h changes sign precisely once, namely at $s = 1$. Thus if $|\nabla u(x, t)| > 1$, then (1.1) is not parabolic near (x, t) but gives rise to a backward heat flow perpendicular to S , although it is a forward, hence smoothing, heat flow along S itself. Backward heat

flows are well known to be highly unstable and smooth initial data may lead to singularities in arbitrarily short time. Even if u^0 is twice differentiable, then (1.1) may not have any weak solution at all [19].

Despite of this discouraging analytical facts, Perona and Malik, and many others, found that numerical approximations of (1.1) do not exhibit significant instabilities. Even better: if computations are carried on for a sufficiently large time interval, the approximations seem to produce piecewise constant solutions giving a simplified image of u^0 preserving sharp boundaries of large brightness variation.

This numerical evidence triggered many attempts to replace (1.1) by nearby versions which, on the one hand side, admit solid analytical foundations in terms of existence and uniqueness theorems, and, on the other hand side, possess essentially the same numerical properties as (1.1), at least for small $t > 0$.

The first, and widely used approach is due to Catté, Lions, Morel, and Coll [9]. They employ a space regularization by replacing ∇u in the argument of g by ∇u_σ , where $u_\sigma := G_\sigma \star \tilde{u}$, with \star denoting convolution with respect to the space variables, G_σ is the Gaussian with variance $\sigma > 0$, and \tilde{u} is an appropriate extension of u over \mathbb{R}^n (by zero, for example). In [9] it is shown that the regularized Perona-Malik problem

$$(1.5) \quad \begin{cases} \partial_t u - \nabla \cdot (g(|\nabla u_\sigma|^2) \nabla u) = 0 & \text{in } \Omega \times (0, \infty), \\ \partial_\nu u = 0 & \text{on } \Gamma \times (0, \infty), \\ u(\cdot, 0) = u^0 & \text{on } \Omega \end{cases}$$

possesses for each $u^0 \in L_2 := L_2(\Omega)$ a unique global weak solution satisfying

$$u \in C([0, T], L_2) \cap L_2((0, T), H^1)$$

for every $T > 0$. (This solution is more regular on $\Omega \times (0, \infty)$, but this is of no importance for our purposes. Thus we do not give details, neither here nor in similar situations.) It depends Lipschitz continuously on u^0 . Furthermore,

$$(1.6) \quad \operatorname{ess\,min} u^0 \leq u(\cdot, t) \leq \operatorname{ess\,max} u^0, \quad t \geq 0,$$

and

$$(1.7) \quad u(\cdot, t) \rightarrow \int_{\Omega} u^0 \, dx := \frac{1}{|\Omega|} \int_{\Omega} u^0 \, dx$$

exponentially fast in L_2 (in fact, in L_p for $1 < p < \infty$) as $t \rightarrow \infty$ (cf. [28, Section 2.4]). Whereas (1.6) is a desirable feature in image processing, (1.7) is not since it means that, in the long run, one obtains a ‘picture’ being uniformly grey and thus containing no information at all. Variants of (1.5) have been proposed and analyzed by many authors (e.g., [12], [28], [15], [16], and the references therein).

At the same time Alvarez, Lions, and Morel [2] investigated the degenerate diffusion equation

$$(1.8) \quad \partial_t u - g(|\nabla u_{\sigma}|) |\nabla u| \operatorname{div} \left(\frac{\nabla u}{|\nabla u|} \right) = 0.$$

Note that

$$(1.9) \quad |\nabla u| \operatorname{div} \left(\frac{\nabla u}{|\nabla u|} \right) = \Delta u - \frac{\nabla u}{|\nabla u|} \cdot D^2 u \frac{\nabla u}{|\nabla u|} = \Delta_S u.$$

Thus in (1.8) there is only diffusion along S and no diffusion perpendicular to it. By comparing (1.3) to (1.9) the relationship between (1.5) and (1.8) is obvious. The regularized edge stopping function $g(|\nabla u_{\sigma}|)$ is introduced in (1.8) in order to prevent shrinking of the level sets, known to occur for the standard mean curvature flow (obtained for $g = 1$). It is shown in [2] that (1.8) possesses a unique global viscosity solution depending Lipschitz continuously

on u^0 and satisfying (1.6). For various variants and modifications of (1.8) we refer to [1], [24], [26], and the references therein.

M. Nitzberg and T. Shiota [21] were the first to propose a space and time regularized version of (1.1). They report, in particular, numerical experiments for the system

$$(1.10) \quad \begin{cases} \partial_t u - \nabla \cdot (g(v)\nabla u) = 0, \\ \partial_t v + \omega v = \omega G_\sigma \star |\nabla u|^2, \end{cases}$$

where $\omega > 0$ is a (relaxation) parameter. Note that the second equation implies that

$$v(\cdot, t) = e^{-\omega t} v^0 + \omega \int_0^t e^{-\omega(t-\tau)} G_\sigma \star |\nabla u(\cdot, \tau)|^2 d\tau, \quad t \geq 0.$$

Set $\vartheta_\omega(t) := \omega e^{-\omega t}$ for $t \geq 0$ and note that $\int_0^\infty \vartheta_\omega(t) dt = 1$. Denoting by \star convolution with respect to $t \geq 0$, it follows that

$$v = \frac{1}{\omega} \vartheta_\omega v^0 + \vartheta_\omega \star (G_\sigma \star |\nabla u|^2).$$

Nitzberg and Shiota consider the limiting case $\sigma = 0$ also, where $G_0 := \delta_0$, the Dirac measure supported in zero. In this case, setting $v^0 = 0$ as well, (1.10) reduces to

$$(1.11) \quad \partial_t u - \nabla \cdot (g(\vartheta_\omega \star |\nabla u|^2)\nabla u) = 0.$$

Thus in this case (1.10) is equivalent to a delay-differential equation obtained from (1.1) by replacing $|\nabla u|^2$ by its weighted average $\vartheta_\omega \star |\nabla u|^2$ which, at time $t > 0$, takes account of the whole history of $|\nabla u|^2$ back to $t = 0$. There is no mathematical justification of (1.10) in [21].

A variant of (1.10) of the form

$$(1.12) \quad \begin{cases} \partial_t u - \nabla \cdot (L\nabla u) = 0, \\ \partial_t L + L = F(\nabla u_\sigma), \end{cases}$$

with F a positive semidefinite $n \times n$ matrix valued function has been studied by Cottet and El Ayyadi [11]. Imposing the strong restriction that F be uniformly bounded in the C^1 norm, the global well posedness of (1.12) is shown in the sense that

$$u \in L_2((0, T), H^1) \cap L_\infty((0, T), L_\infty), \quad T > 0.$$

It is essential that $\sigma > 0$.

Y. Chen and P. Bose [10] consider nonlinear diffusion filters based on

$$(1.13) \quad \begin{cases} \partial_t u - g(v) |\nabla u| \operatorname{div} \left(\frac{\nabla u}{|\nabla u|} \right) - \nabla g(v) \cdot \nabla u = \lambda |\nabla u| (u - u^0), \\ \partial_t v + \omega v = \omega |\nabla u_\sigma|. \end{cases}$$

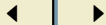
They prove that (1.13), complemented by no-flux boundary conditions, possesses a unique global viscosity solution depending Lipschitz continuously on u^0 and satisfying (1.6). Again the assumption that $\sigma > 0$ is crucial.

The space regularizations ∇u_σ and $G_\sigma \star |\nabla u|^2$, employed to replace the ill posed Perona-Malik model by a mathematical sound one, produce an undesirable smoothing of sharp edges which, in principle, are supposed to be enhanced by the filters. This is due to the fact that $\nabla u_\sigma = G_\sigma \star \nabla u$ and $G_\sigma \star |\nabla u|^2$ are weighted averages of ∇u and $|\nabla u|^2$, respectively. Even if a small value of σ is chosen so that most of the mass of G_σ is concentrated near 0, for the evaluation of the convolution integral $G_\sigma \star \nabla u$ the behavior of ∇u in a full neighborhood of a given point x is taken into account. Thus if x is a point on a sharp edge, where $|\nabla u|$ varies relatively abruptly from small size on one side of the edge to large values on the other side, this variation is diminished by replacing $|\nabla u|^2$ by $|\nabla u_\sigma|^2$. Thus, on the average, the diffusion coefficient $g(|\nabla u_\sigma|^2)$ is bigger than $g(|\nabla u|^2)$, the one of the Perona-Malik model, resulting in faster diffusion, hence stronger smoothing.

Home Page

Title Page

Contents



Page 19 of 52

Go Back

Full Screen

Close

Quit

It is clear that this smoothing effect has to occur also in numerical approximations based on space regularized models. Indeed, any discretization of the convolution term ∇u_σ has to be a weighted average of (the corresponding discretization of) ∇u . Thus large variations of ∇u are leveled out in the discrete case as well. This is illustrated by numerical experiments where a noisy picture of a cameraman (Figures 1 and 2) has been processed by a Catté-Lions-Morel-Coll (henceforth abbreviated by CLMC) filter (1.5) (see Figures 3 and 4).

In Figures 2 and 4 three-dimensional plots of the corresponding grey level distributions $u(\cdot, 0)$ and $u(\cdot, 0.05)$ are shown, where the value 1 of u corresponds to white and 0 to black. The smoothing of the edges is particularly well seen in the center part of Figure 4. (We refer to Section 2 for details on the numerical implementation.) For the purpose of illustration we have chosen a relatively large value of σ . It is clear that the smoothing effect is less pronounced for smaller values of σ . But due to the very nature of weighted space averaging, it cannot be avoided completely (see Section 2 below).

As explained above, similar effects have to occur necessarily in the modified mean curvature flow (1.8). There the strong smoothing effect of the usual mean curvature flow is further enhanced by the space convolution smoothing ∇u_σ employed in the edge stopping function.

For these reasons it is desirable to avoid spatial smoothing at all and look for other regularizations of the Perona-Malik equations. A first step in this direction has been made by A. Belahmidi [7] and Belahmidi and Chambolle [8] who were concerned with the Nitzberg-Shiota model (1.10) in the limit case $\sigma = 0$. More precisely, these authors study the system

$$(1.14) \quad \begin{cases} \partial_t u - \nabla \cdot (g(v)\nabla u) = 0, \\ \partial_t v + v = F(|\nabla u|^2) \end{cases}$$

Home Page

Title Page

Contents



Page 20 of 52

Go Back

Full Screen

Close

Quit



Fig. 1

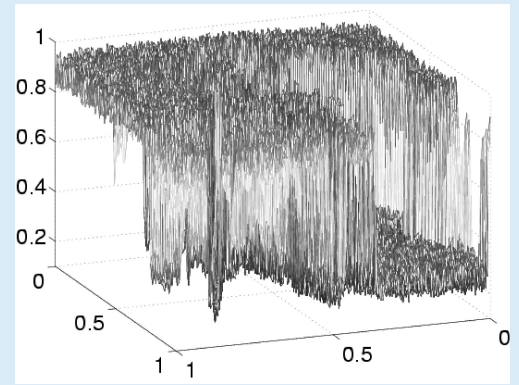


Fig. 2

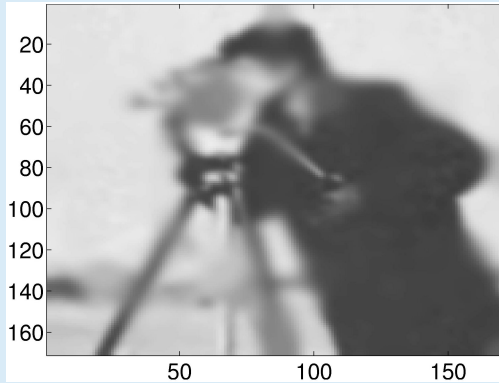


Fig. 3

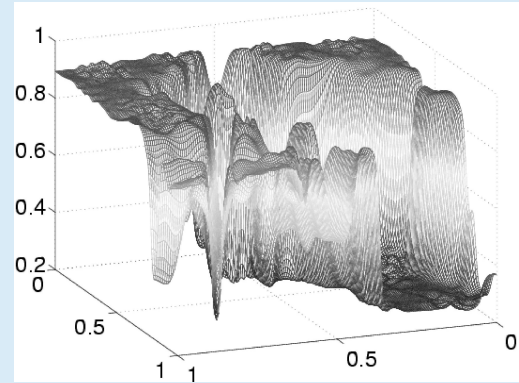


Fig. 4



with no-flux boundary conditions. In [7] it is shown that, given $\alpha \in (0, 1)$ and any initial datum

$$(u^0, v^0) \in C^{2+\alpha}(\bar{\Omega}) \times C^{1+\alpha}(\bar{\Omega}), \quad v^0 \geq 0,$$

there exists a unique maximal solution (u, v) of (1.14) such that $u, \nabla u, D^2u, u_t, v$, and ∇v are α Hölder continuous with respect to the standard parabolic metric of $\Omega \times [0, T_{\max})$. Of course, Ω has to be of class $C^{2+\alpha}$ and F is supposed to satisfy $F(0) = 0$ and to belong to $C^{3-}(\mathbb{R}^+, \mathbb{R}_+)$, where, in general, $C^{(k+1)-}$ is the space of all k times continuously differentiable functions whose k -th derivatives are (locally) Lipschitz continuous. Thus $F(s) := s$ is admissible for $s \geq 0$, in which case (1.14) reduces to the Nitzberg-Shiota model (1.10) with $\sigma = 0$. In [8] it is shown that (1.14) has a global weak solution (there is no uniqueness proof)

$$(u, v) \in (H^1(Q_T) \cap L_\infty(Q_T))^2, \quad T > 0,$$

where $Q_T := \Omega \times (0, T)$, given the strong hypotheses that F be uniformly bounded and $n = 2$ (which is essential for the proof and rules out the Nitzberg-Shiota model).

Numerical experiments reported in [7], [8], as well as in [21] indicate that sharp edges are well preserved over rather long time intervals. The same is even more true for numerical experiments with the original Perona-Malik equations.

Why does the Perona-Malik model – though mathematically ill posed – produce extremely convincing numerical results with an ‘unreasonable effectiveness’ [17]? A hint for the understanding of this fact comes from the numerical implementations of (1.1). For this we write (1.1) formally as a quasilinear evolution equation

$$(1.15) \quad \dot{u} + A(u)u = 0 \quad \text{in } (0, \infty), \quad u(0) = u^0.$$

In all numerical calculations we are aware of, an implicit Euler scheme (of step-size δ) is used to approximate the time derivative. Setting $u^k := u(k\delta)$ for $k \in \mathbb{N}$, we end up with a

semidiscrete scheme of the form

$$(1.16) \quad u^{k+1} - u^k + \delta A(u^k)u^{k+1} = 0, \quad k \in \mathbb{N}.$$

The crucial observation is now the fact that, instead of the natural expression $A(u^{k+1})u^{k+1}$, the linearized version $A(u^k)u^{k+1}$ is used. In other words, a memory effect of the nonlinear term is built into the time discretized equations. Since, due to the ill posedness of (1.1), it cannot be expected that a limiting argument, as $\delta \rightarrow 0$, will produce a solution smooth enough to write down (1.1) in its natural weak form, *it may as well be the case that (1.16) corresponds to a (non linearized) time discretization of a time-delayed Perona-Malik problem*

$$(1.17) \quad \begin{cases} \partial_t u - \nabla \cdot (g(\theta * |\nabla u|^2) \nabla u) = 0 & \text{on } \Omega \times (0, \infty), \\ \partial_\nu u = 0 & \text{on } \Gamma \times (0, \infty), \\ u = u^0 & \text{on } \Omega \times (-S, 0]. \end{cases}$$

In fact, set $S := 2\delta$ and $\theta := \chi_{(0,S)}/S$, where $\chi_{(0,S)}$ is the characteristic function of the interval $(0, S)$. Then

$$(1.18) \quad \theta * |\nabla u|^2(t) = \int_{t-S}^t |\nabla u(\tau)|^2 d\tau, \quad t \geq 0.$$

Thus, by discretizing this integral by the midpoint rule, we see that

$$\theta * |\nabla u|^2((k+1)\delta) \sim |\nabla u^k|^2,$$

so that we arrive at (1.16) in this case also. In other words, *by looking at (1.16), it cannot be decided whether this system results from a discretization of the local equation (1.15) or of the time-delayed problem.*

It should be observed that in the convolution integral (1.18) no space averaging occurs. At a given point (x, t) only values of $|\nabla u|^2$ at earlier time instances $\tau \in [t - T, t]$, but *at the*



same space point x , are taken into account. Thus it is to be expected that, as times increases, the diffusion coefficient $g(\theta * |\nabla u|^2)$ will vary only slowly due to the diffusive motion of u . This will produce only little smoothing of sharp edges, much less than the space averaging process. It is also clear that the diffusive effects on the ‘edge stopping function’ g can be made small if the support of θ is small and most weight is put near zero, so that θ is a close approximation of the Dirac measure δ_0 (see Section 2 for numerical experiments).

By these considerations we are led to study time-delayed Perona-Malik equations of the form (1.17). In order to present our main result we first introduce some notation. We set $J_T := [0, T)$ for $0 < T \leq \infty$ and

$$H_{q, \partial_\nu}^2 := \{u \in H_q^2; \partial_\nu u = 0\}, \quad 1 < q < \infty,$$

where $H_q^2 := H_q^2(\Omega)$, etc. Furthermore,

$$\mathcal{H}(Q_T) := \mathcal{H}_{q,p,\partial_\nu}^{2,1}(Q_T) := L_p(J_T, H_{q,\partial_\nu}^2) \cap H_p^1(\overset{\circ}{J}_T, L_q), \quad p, q \in (1, \infty).$$

Then we assume that

$$(1.19) \quad \begin{cases} \Omega \text{ is of class } C^2; \\ 2/p + n/q < 1. \end{cases}$$

It follows (see (3.4)) that

$$(1.20) \quad \mathcal{H}(Q_T) \hookrightarrow C(\bar{J}_T, C^1(\bar{\Omega})), \quad 0 < T < \infty.$$

Theorem 1.1. *Let assumption (1.19) be satisfied and suppose that g belongs to $C^2(\mathbb{R}^+, (0, \infty))$. Also suppose that $\theta \in L_s(J_S, \mathbb{R}^+)$ for some $s > 1$ and $0 < S < \infty$, and that $u^0 \in H_{q,\partial_\nu}^2$. Then:*

- (i) *There exists a maximal $T^* \in (0, \infty]$ such that (1.17) possesses a unique solution u^* on J_{T^*} such that $u \in \mathcal{H}(Q_T)$ for $0 < T < T^*$.*
- (ii) *If $T^* < \infty$, then $u^* \notin \mathcal{H}(Q_{T^*})$.*



- (iii) If $\text{supp}(\theta) \subset [\sigma, S]$ for some $\sigma \in (0, S)$, then $T^* = \infty$.
 (iv) Fix $T \in (0, T^*)$ and let (u_j^0, θ_j, g_j) be a sequence in

$$(1.21) \quad H_{q, \partial_\nu}^2 \times L_s(J_S, \mathbb{R}^+) \times C^{2^-}(\mathbb{R}^+, (0, \infty))$$

converging towards (u^0, θ, g) . Denote by u_j^* the unique maximal solution of (1.17) with (u^0, θ, g) replaced by (u_j^0, θ_j, g_j) , and let T_j^* be the corresponding maximal existence time. Then $T_j^* > T$ for all sufficiently large j , and $u_j^* \rightarrow u^*$ in $\mathcal{H}(Q_T)$ as $j \rightarrow \infty$.

- (v) For $0 \leq t < T^*$,

$$\min u^0 \leq u^*(\cdot, t) \leq \max u^0.$$

- (vi) For $0 \leq t < T^*$,

$$\int_{\Omega} u^*(x, t) \, dx = \int_{\Omega} u^0(x) \, dx.$$

- (vii) For $0 \leq t < T^*$ and $2 \leq s \leq \infty$,

$$\left\| u^*(\cdot, t) - \int_{\Omega} u^0 \, dx \right\|_{L_s} \leq \left\| u^0 - \int_{\Omega} u^0 \, dx \right\|_{L_s}.$$

The proof of this theorem is given in Section 5.

Remarks 1.2. (a) Of course, (1.21) is endowed with the obvious topology such that convergence of g_j towards g means that

$$\|g_j - g\|_{L_\infty(B)} + \|\nabla g_j - \nabla g\|_{L_\infty(B)} + [\nabla g_j - \nabla g]_B \rightarrow 0$$

for every bounded interval B in \mathbb{R}^+ , where $[\cdot]_B$ is the Lipschitz seminorm on B .

- (b) It follows from (ii) and (v) that

$$\limsup_{t \uparrow T^*} (\|\nabla u^*(\cdot, t)\|_{L_q} + \|D^2 u^*(\cdot, t)\|_{L_q} + \|\dot{u}^*(\cdot, t)\|_{L_q}) = \infty$$

if $T^* < \infty$, whereas u^* stays uniformly bounded. We expect that, in fact, the gradient of u^* blows up if $T^* < \infty$, at least if (1.17) is a close approximation of (1.1), that is, if θ is a good approximation of the Dirac measure δ_0 . This conjecture is supported by a result of Kawohl and Kutev [18] who showed, in the one-dimensional case, that there are initial values satisfying $|\nabla u^0(x)| > 1$ on a sufficiently large subset of Ω such that (1.1) has no global weak C^1 solution.

(c) For each $T \in (0, T^*)$ there exists $\alpha = \alpha(T) > 0$ such that

$$\left\| u^*(\cdot, t) - \int_{\Omega} u^0 \, dx \right\|_{L_2} \leq e^{-\alpha t} \left\| u^0 - \int_{\Omega} u^0 \, dx \right\|_{L_2}, \quad 0 \leq t \leq T.$$

If

$$(1.22) \quad g(\theta * |\nabla u^*|(t)) \geq \beta > 0, \quad 0 \leq t < T^*,$$

then α can be chosen to be independent of $T \in (0, T^*)$. Thus if $T^* = \infty$ and (1.22) holds, which is true, in particular, if $g(\xi) \geq \beta > 0$ for $\xi \in \mathbb{R}^+$, then $u^*(\cdot, t)$ converges to the constant value $\int_{\Omega} u^0 \, dx$ as $t \rightarrow \infty$. Of course, this is an undesirable case for image processing since it means, as noted earlier, that in the long run a uniformly grey image is obtained. \square

2. NUMERICAL EXPERIMENTS

To illustrate the potential power of the proposed time-delayed approach we describe numerical experiments carried out with the noisy image of the cameraman (Figures 1 and 2; the rectangular shape of the image should be considered as an approximation of a smooth domain, of course. Similarly, the smooth initial values of Theorem 1.1 are to be considered as being approximations for piece-wise constant functions. The problem of error estimates is not addressed in this paper). In all these calculations a continuous piecewise affine finite element

method has been applied for space discretization. For this each side of the picture has been subdivided into 172 equal intervals and the resulting rectangular net has been triangulated by the first diagonal.

In Figures 3 and 4 time-step $\delta = 10^{-2}$ and variance $\sigma = 0.361$ have been used and $k = 5$ time-steps were carried out, applying, as usual, iteration method (1.16). Following [9], the convolution $u_\sigma = G_\sigma \star u$ has been approximated by a finite element solution of the heat equation at time $\sigma^2/2$ with initial value $\tilde{u}(\cdot, t)$, where \tilde{u} is the extension of $u(\cdot, t)$ by reflection. Since $t = k \cdot \delta = 5 \cdot 10^{-2} \sim \sigma^2/2$, the criterion suggested in [9] for relating σ and k is satisfied.

We repeat that the relatively large value of σ is chosen for demonstrating clearly the smoothing effect of space convolution. Of course, in concrete situations a smaller σ is appropriate (e.g., [20], [28]). Below (see Fig. 13) we use a much smaller, more realistic value for σ in order to compare the CLMC space regularization method with the proposed time regularization technique.

For the choice of θ in the time-delayed method we introduced, besides of the time-step δ , a parameter $\alpha \geq 0$ and set

$$\theta(t) := \theta_{\alpha, \delta}(t) := \vartheta_\alpha(t/\delta)/\delta, \quad 0 \leq t \leq \delta,$$

where ϑ_α is defined by

$$\vartheta_\alpha(t) := 2(1 + \alpha - \alpha t)/(2 + \alpha), \quad 0 \leq t \leq 1.$$

Hence $\theta \in L_\infty(0, \delta)$, satisfies $\theta \geq 0$ and $\int \theta dt = 1$, and approaches the Dirac distribution as $\delta \rightarrow 0$. With this choice the convolution integral

$$(2.1) \quad \theta * |\nabla u|^2(t) = \int_{t-\delta}^t \theta(t-\tau) |\nabla u(\tau)|^2 d\tau$$

has been approximated by the one-step trapezoidal rule resulting in the weighted mean

Home Page

Title Page

Contents



Page 27 of 52

Go Back

Full Screen

Close

Quit



Fig. 5

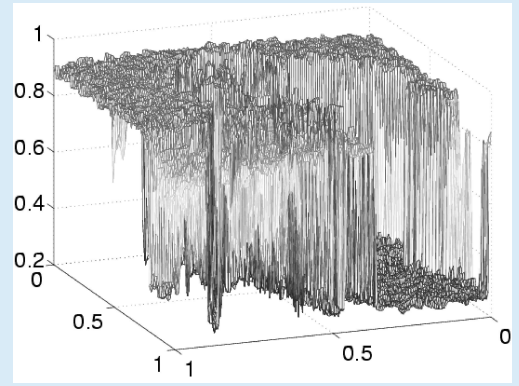


Fig. 6



Fig. 7

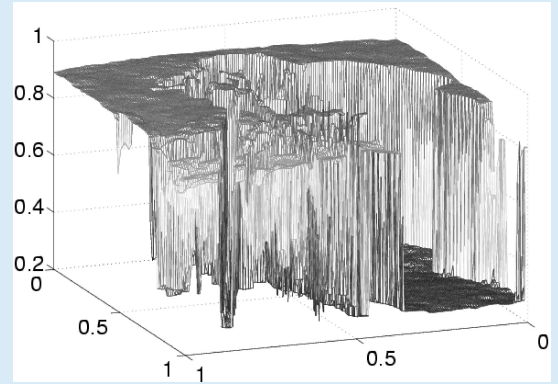


Fig. 8

Home Page

Title Page

Contents



Page 28 of 52

Go Back

Full Screen

Close

Quit

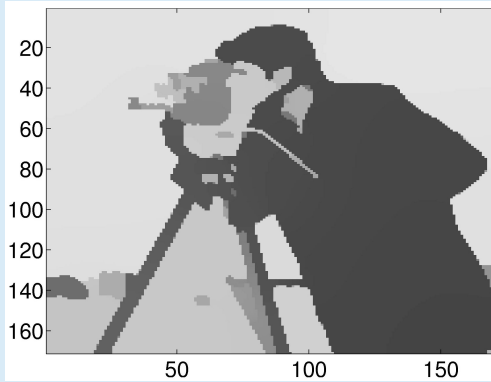


Fig. 9

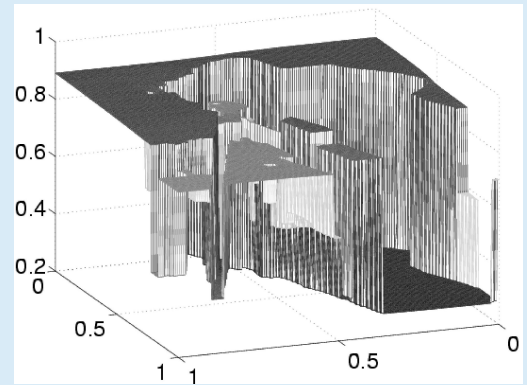


Fig. 10

To increase the value of α means to use a better approximation of the Dirac distribution, thus to be closer to the original Perona-Malik model. From (2.2) one sees that a large value of α places a high weight on the value of $|\nabla u|^2$ at time t , the actual level of computation, and only a very small one on $|\nabla u(t - \delta)|^2$. Thus it is to be expected that, using a larger value of α , fewer steps will lead to a sharp image. This is seen by comparing Figures 6 and 11, where in the latter the result of the computation with $\alpha = 100$ and $k = 1$ is plotted.

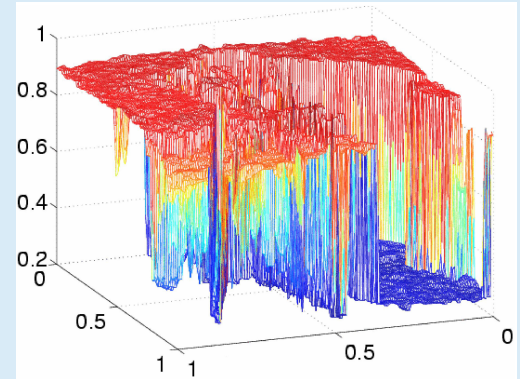


Fig. 11

$$(2.2) \quad \frac{(1 + \alpha) |\nabla u(t)|^2 + |\nabla u(t - \delta)|^2}{2 + \alpha}.$$

All computations described below used time discretization $\delta = 10^{-3}$.

In Figures 5–10 we exhibit numerical results obtained by choosing $\alpha = 10$ and carrying out $k = 1$ (in Figures 5 and 6), $k = 2$ (in Figures 7 and 8), and $k = 50$ (in Figures 9 and 10) iteration steps.

Since $t = 50 \cdot 10^{-3} = 5 \cdot 10^{-2}$, Figures 9 and 10 can be compared to Figures 3 and 4. This comparison shows clearly that the time-delayed approach preserves sharp edges much better than the space convolution technique.

Figure 12 shows the numerical finding for the case $\alpha = 100$ and $k = 3$.

This should be compared to Figure 13 where the outcome CLMC method with $k = 3$ and $\sigma = 0.00003162$ is depicted. The small value of σ has been chosen in order that ∇u_σ be a good approximation of ∇u , so that the model is close to the Perona-Malik system as well.

Figure 13 shows again the undesirable smoothing of the edges (in the center part of the figure) due to space convolution. This is seen even better in Figure 14, where the one-dimensional section along the dark line in Figure 15 has been plotted for $\alpha = 100$ ('time') versus the CLMC model ('space'), after $k = 5$ steps for each.

In Figure 16 the one-dimensional sections for $\alpha = 100$ and $k = 1$ and 3 are given in order to illustrate the fact that by our method the positions of the sharp edges are rather stable.

Home Page

Title Page

Contents



Page 30 of 52

Go Back

Full Screen

Close

Quit

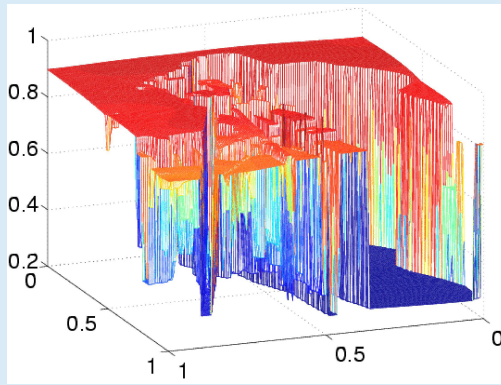


Fig. 12

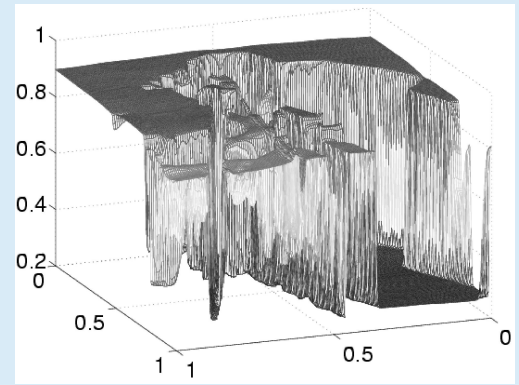


Fig. 13

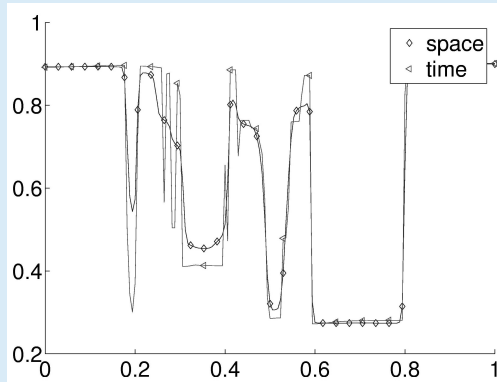


Fig. 14

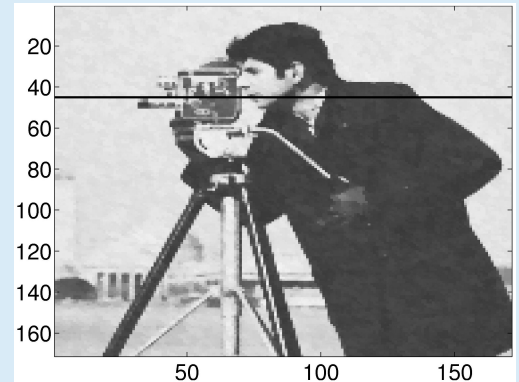


Fig. 15

Home Page

Title Page

Contents



Page 31 of 52

Go Back

Full Screen

Close

Quit

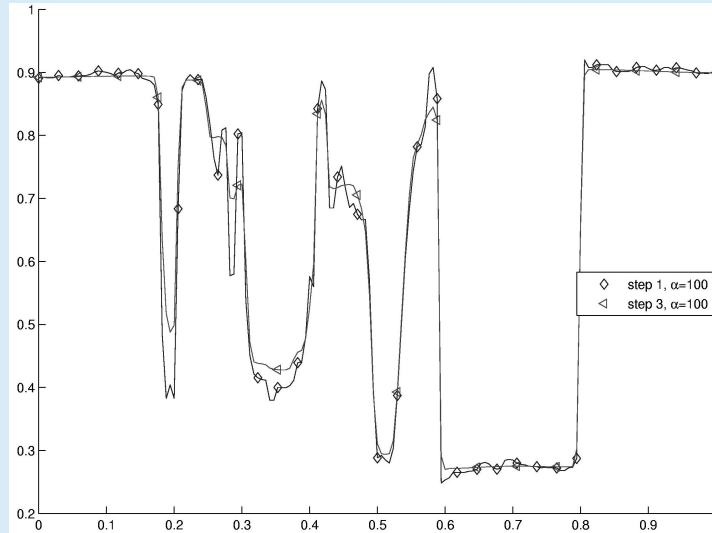


Fig. 16

Figure 17 illustrates the fact that higher values of α lead faster to sharper images than smaller ones. One-dimensional sections are plotted for the values $\alpha = 0$ and $\alpha = 100$ with $k = 1$.

Home Page

Title Page

Contents



Page 32 of 52

Go Back

Full Screen

Close

Quit

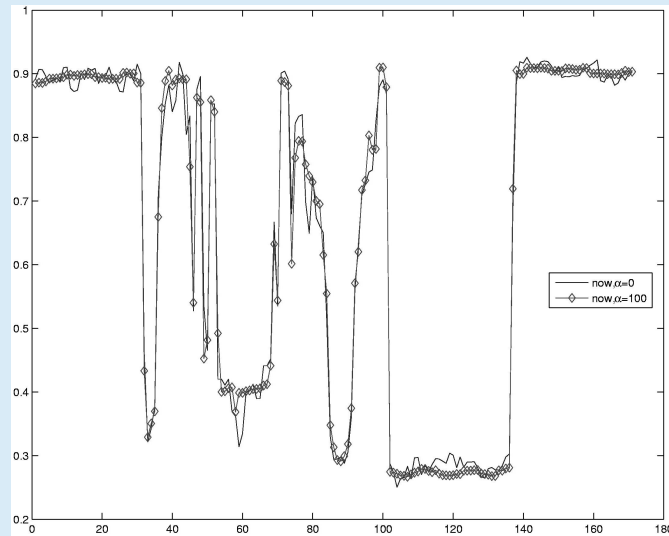


Fig. 17

In all the numerical computations described above, based on the time-delayed model, at each step k there has to be solved a nonlinear discrete equation of the form

$$(2.3) \quad u^{k+1} + \delta M(u^{k+1}, u^k)u^{k+1} = u^k$$

for u^{k+1} which is obtained by using (2.2) as an approximation for (2.1) and, in addition, a (finite element) space discretization. In the reported calculations, (2.3) has been approximately solved by a standard Banach fixed point iteration carrying out 3 iteration steps (by which the discrete ℓ_2 norm of the difference between the second and the third approximation became smaller than 10^{-3}).

Solving at each time-step k a nonlinear equation of the form (2.3) can be avoided if (2.2) is replaced by

$$(2.4) \quad \frac{(1 + \alpha) |\nabla u(t - \delta)|^2 + \alpha |\nabla u(t - 2\delta)|^2}{2 + \alpha}.$$

This amounts to shifting θ by δ to the right, that is, by replacing θ by $t \mapsto \theta(t - \delta)$. In this case (2.3) has to be replaced by the linear equation

$$u^{k+1} + \delta M(u^k, u^{k-1})u^{k+1} = u^k$$

for u^{k+1} . Besides of simplifying the numerical computations, this method has the additional advantage that Theorem 1.1 guarantees the solution of (1.17) to exist globally, since condition (iii) is now satisfied with $\sigma := \delta$ and $S := 2\delta$. However, it is to be expected that this method will not produce results of the same quality as the one using (2.2) since the ‘past’ plays now a much more important role.

Indeed, this is illustrated by Figures 18–21, where we have chosen $k = 1$ (Figures 18 and 19) and $k = 3$ (Figures 20 and 21). Figures 18 and 20 have been computed by using (2.2), and Figures 19 and 21 by employing (2.4), setting $\alpha = 100$ in either case.

Home Page

Title Page

Contents



Page 34 of 52

Go Back

Full Screen

Close

Quit

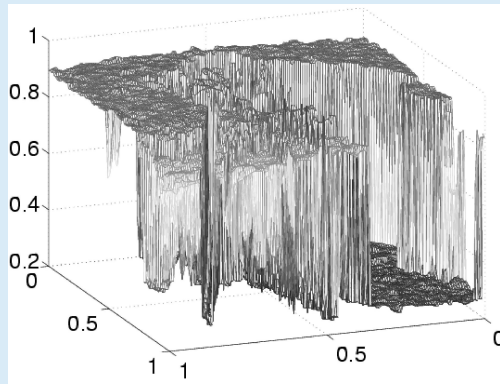


Fig. 18

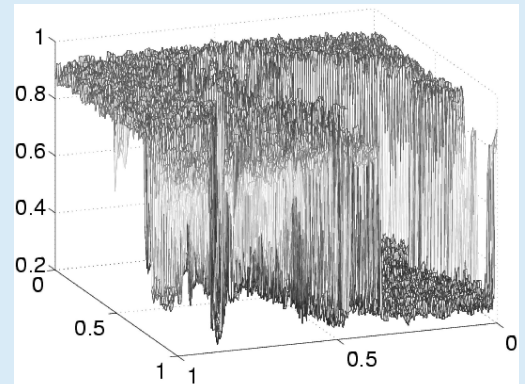


Fig. 19

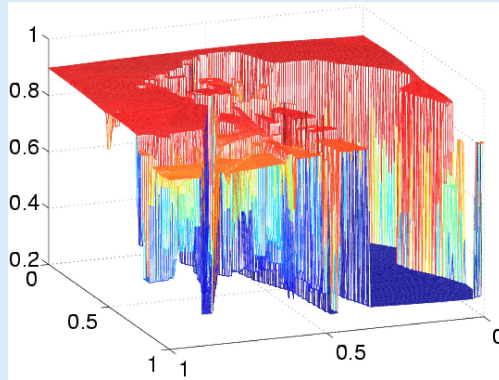


Fig. 20

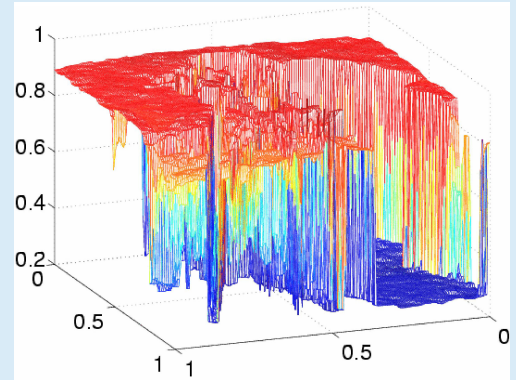


Fig. 21

3. PRELIMINARIES

Throughout this section we suppose that

$$(3.1) \quad \begin{cases} \text{assumption (1.19) holds;} \\ \Gamma = \Gamma_0 \cup \Gamma_1 \text{ with } \Gamma_0 \cap \Gamma_1 = \emptyset \text{ and } \Gamma_0 \text{ being open and closed in } \Gamma. \end{cases}$$

Note that either Γ_0 or Γ_1 may be empty. We denote by χ the characteristic function of Γ_1 , by γ the trace operator, and set $\mathcal{B} := \chi\partial_\nu + (1 - \chi)\gamma$. Then we put

$$H_{q,\mathcal{B}}^2 := \{v \in H_q^2 ; \mathcal{B}v = 0\}.$$

We write I for an interval containing more than one point and set

$$\mathcal{H}(\Omega \times I) := \mathcal{H}_{q,p,\mathcal{B}}^{2,1}(\Omega \times I) := L_p(I, H_{q,\mathcal{B}}^2) \cap H_p^1(\overset{\circ}{I}, L_q).$$

Furthermore, $B_{q,p}^s := B_{q,p}^s(\Omega)$ are the usual Besov spaces of order $s \in (0, 2)$, and

$$B_{q,p,\mathcal{B}}^{2-2/p} := \{v \in B_{q,p}^{2-2/p} ; \mathcal{B}v = 0\}.$$

Then, except for equivalent norms,

$$(3.2) \quad (L_q, H_{q,\mathcal{B}}^2)_{1/p', p} = B_{q,p,\mathcal{B}}^{2-2/p},$$

with $(\cdot, \cdot)_{\theta, p}$ denoting the real interpolation functor of exponent $\theta \in (0, 1)$ and parameter p (cf. [3, Theorem 5.2]). Observe that

$$(3.3) \quad H_{q,\mathcal{B}}^{s_1} \xrightarrow{d} B_{q,p,\mathcal{B}}^{2-2/p} \xrightarrow{d} H_{q,\mathcal{B}}^{s_0}, \quad 1 + 1/q < s_0 < 2 - 2/p < s_1 \leq 2,$$

where H_q^s are the usual Bessel potential spaces of order $s \in [0, 2]$ over Ω (so that $H_q^0 = L_q$), and

$$H_{q,\mathcal{B}}^s = \{v \in H_q^s ; \mathcal{B}v = 0\}, \quad 1 + 1/q < s \leq 2.$$

Since $2 - 2/p > 1 + n/q$, a well known Sobolev type embedding theorem guarantees that, setting $\rho := 1 - 2/p - n/q$,

$$B_{q,p,\mathcal{B}}^{2-2/p} \hookrightarrow C_B^{1+\rho}(\bar{\Omega}) := \{v \in C^{1+\rho}(\bar{\Omega}) ; \mathcal{B}v = 0\}.$$

Thus (3.2) and the trace theorem imply (cf. [4, Theorem III.4.10.2]) that

$$(3.4) \quad \mathcal{H}(\Omega \times I) \hookrightarrow C_0\left(\bar{I}, B_{q,p,\mathcal{B}}^{2-2/p}\right) \hookrightarrow C_0\left(\bar{I}, C^{1+\rho}(\bar{\Omega})\right) \hookrightarrow C_0\left(\bar{I}, C^1(\bar{\Omega})\right),$$

where C_0 is the space of continuous functions vanishing at infinity.

Suppose that $1 \leq s \leq \infty$ and E is a Banach space. Then we identify $L_s(I, E)$ with a closed linear subspace of $L_s(\mathbb{R}, E)$ by identifying $v \in L_s(I, E)$ with its extension by zero outside I , its trivial extension. Consequently, given $\omega \in L_s(\mathbb{R}^+)$ and $v \in L_p(I, E)$, the convolution product $\omega * v$ is well defined and given by

$$\omega * v(t) = \int_{I \cap [\tau \leq t]} \omega(t - \tau)v(\tau) \, d\tau = \int_{(t-I) \cap \mathbb{R}^+} \omega(\tau)v(t - \tau) \, d\tau, \quad t \in \mathbb{R}.$$

From Young's inequality and well known properties of convolutions we infer that $(\omega, v) \mapsto \omega * v$ defines continuous bilinear maps

$$(3.5) \quad L_s(\mathbb{R}^+) \times L_{s'}(I, E) \rightarrow C_0(\mathbb{R}, E)$$

and

$$(3.6) \quad L_s(\mathbb{R}^+) \times L_p(I, E) \rightarrow L_r(\mathbb{R}, E),$$

provided

$$(3.7) \quad \frac{1}{s} + \frac{1}{p} = 1 + \frac{1}{r}.$$

Given a second Banach space F , we denote by $\mathcal{C}^{1-}(E, F)$ the Fréchet space of all maps from E into F being uniformly Lipschitz continuous on bounded sets, endowed with its natural topology of uniform convergence on bounded sets of the functions and their difference quotients. Note that $\mathcal{C}^{1-}(E, F) = \mathcal{C}^1(E, F)$ if E is finite dimensional.

Henceforth, we suppose that

$$(3.8) \quad \begin{cases} k, m \in \mathbb{N}^\times := \mathbb{N} \setminus \{0\} \text{ and } \alpha \in C^{2-}(\mathbb{R}^n, \mathbb{R}^m); \\ 1 \leq s \leq p', \quad 0 < S \leq \infty; \\ \omega \in L_1 \cap L_s(J_S, \mathcal{L}(\mathbb{R}^m, \mathbb{R}^k)); \\ r \text{ is defined by (3.7).} \end{cases}$$

We fix $T > 0$ and put

$$J := -J_S \cup J_T = (-S, T).$$

Given $\bar{u} : -J_S \rightarrow E$ and $u : J_T \rightarrow E$, we define $\bar{u} \oplus u : J \rightarrow E$ by

$$\bar{u} \oplus u(t) := \begin{cases} \bar{u}(t), & -S < t < 0, \\ u(t), & 0 \leq t < T. \end{cases}$$

We also define the *history space* \mathcal{H}^- by

$$\mathcal{H}^- := \mathcal{H}(\Omega \times (-J_S))$$

and set $\mathcal{H} := \mathcal{H}(\Omega \times J_T)$. It follows easily from (3.4) and $\mathcal{H}(\Omega \times I) \hookrightarrow L_p(I, H_{q,B}^2)$ that

$$(3.9) \quad ((\bar{u}, u) \mapsto \bar{u} \oplus u) \in \mathcal{C}^{1-}(\mathcal{H}^- \times \mathcal{H}, L_\infty(J, C^{1+\rho}(\bar{\Omega})) \cap L_p(J, H_{q,B}^2)).$$

In fact, since $\bar{u} \oplus u - \bar{v} \oplus v = (\bar{u} - \bar{v}) \oplus (u - v)$, we see that (3.9) is even globally Lipschitz continuous.

Put

$$\mathbf{A}(\bar{u}, u) := \omega * \alpha(\nabla \bar{u} \oplus \nabla u), \quad (\bar{u}, u) \in \mathcal{H}^- \times \mathcal{H}.$$

It is a consequence of (3.4)–(3.9) that

$$\partial_j \mathbf{A}(\bar{u}, u) = \omega * (\partial \alpha(\nabla \bar{u} \oplus \nabla u)(\nabla \partial_j \bar{u} \oplus \nabla \partial_j u)), \quad 1 \leq j \leq n,$$

and

$$(3.10) \quad \mathbf{A} \in C^{1-}(\mathcal{H}^- \times \mathcal{H}, C_0(\bar{J}, C(\bar{\Omega}, \mathbb{R}^k)) \cap L_r(J, H_q^1(\Omega, \mathbb{R}^k)))$$

for $(\bar{u}, u) \in \mathcal{H}^- \times \mathcal{H}$.

Finally, we assume that

$$(3.11) \quad a \in C^{2-}(\bar{\Omega} \times \mathbb{R} \times \mathbb{R}^k, (0, \infty))$$

and put

$$\mathbf{a}(\bar{u}, u) := a(\cdot, u, \mathbf{A}(\bar{u}, u)), \quad (\bar{u}, u) \in \mathcal{H}^- \times \mathcal{H}.$$

It follows from (3.4), (3.10), and (3.11) that

$$(3.12) \quad \mathbf{a}(\bar{u}, \cdot) \in C^{1-}(\mathcal{H}, C(\bar{J}_T, C(\bar{\Omega})) \cap L_r(J_T, H_q^1))$$

for $\bar{u} \in \mathcal{H}^-$, since

$$\begin{aligned} \partial_j \mathbf{a}(\bar{u}, u) &= \partial_j a(\cdot, u, \mathbf{A}(\bar{u}, u)) + \partial_{n+1} a(\cdot, u, \mathbf{A}(\bar{u}, u)) \partial_j u \\ &\quad + D_3 a(\cdot, u, \mathbf{A}(\bar{u}, u)) \partial_j \mathbf{A}(\bar{u}, u) \end{aligned}$$

for $j = 1, \dots, n$ and $u \in \mathcal{H}$, with $D_3 a(x, \xi, \eta) \in \mathcal{L}(\mathbb{R}^k, \mathbb{R})$ being the derivative of $a(x, \xi, \cdot) \in C^1(\mathbb{R}^k, \mathbb{R})$ at $\eta \in \mathbb{R}^k$ for $(x, \xi) \in \bar{\Omega} \times \mathbb{R}$. Consequently, setting

$$F_0(\bar{u}, u) := -\nabla \mathbf{a}(\bar{u}, u) \cdot \nabla u, \quad (\bar{u}, u) \in \mathcal{H}^- \times \mathcal{H},$$



and employing (3.4) once more, we see that

$$(3.13) \quad F_0(\bar{u}, \cdot) \in C^{1-}(\mathcal{H}, L_r(J_T, L_q)), \quad \bar{u} \in \mathcal{H}^-.$$

By replacing \mathcal{H} by \mathcal{H}^- in the preceding arguments it similarly follows that

$$\mathbf{a}(\cdot, u) \in C^{1-}(\mathcal{H}^-, C(\bar{J}_T, C(\bar{\Omega})))$$

and

$$F_0(\cdot, u) \in C^{1-}(\mathcal{H}^-, L_r(J_T, L_q))$$

for $u \in \mathcal{H}$.

Also note that the Hölder embedding in (3.4) implies that

$$(3.14) \quad \mathbf{a}(\bar{u}, u) \in C(\bar{J}_T, C^\rho(\bar{\Omega}))$$

for $\bar{u} \in \mathcal{H}^-$ and $u \in \mathcal{H}(\Omega \times J_T)$.

4. MAIN THEOREMS

Throughout this section we suppose that

- assumption (3.1) is satisfied.

We also suppose that

$$(4.1) \quad \left\{ \begin{array}{l} \bullet \quad k, m \in \mathbb{N}^\times, \quad s \in (1, \infty], \quad S \in (0, \infty]; \\ \bullet \quad \omega \in L_1 \cap L_s(J_S, \mathcal{L}(\mathbb{R}^m, \mathbb{R}^k)); \\ \bullet \quad \alpha \in C^{2-}(\mathbb{R}^n, \mathbb{R}^m); \\ \bullet \quad a \in C^{2-}(\bar{\Omega} \times \mathbb{R} \times \mathbb{R}^k, (0, \infty)); \\ \bullet \quad f \in C^{1-}(\bar{\Omega} \times \mathbb{R} \times \mathbb{R}^n); \\ \bullet \quad f_0 \in L_p(\mathbb{R}^+, L_q). \end{array} \right.$$

Then we consider the time-delayed evolution problem:

$$(4.2) \quad \left\{ \begin{array}{ll} \partial_t u - \nabla \cdot (a(\cdot, u, \omega * \alpha(\nabla u)) \nabla u) = f(\cdot, u, \nabla u) + f_0 & \text{on } \Omega \times (0, \infty), \\ u = 0 & \text{on } \Gamma_0 \times (0, \infty), \\ \partial_\nu u = 0 & \text{on } \Gamma_1 \times (0, \infty), \\ u(\cdot, 0) = u^0 & \text{on } \Omega, \\ u = \bar{u} & \text{on } \Omega \times (-S, 0), \end{array} \right.$$

where

$$(4.3) \quad (u^0, \bar{u}) \in B_{q,p,\mathcal{B}}^{2-2/p} \times \mathcal{H}(\Omega \times (-S, 0)).$$

By a **solution**, more precisely, an $\mathcal{H}_{q,p}^{2,1}$ **solution** of (4.2) on J_T , where $0 < T \leq \infty$, we mean a function

$$u : \Omega \times (-S, T) \rightarrow \mathbb{R}$$

such that $u|_{\Omega \times (-J_S)} = \bar{u}$, $u(\cdot, 0) = u^0$, $u|_{Q_\tau} \in \mathcal{H}(Q_\tau)$ for $0 < \tau < T$, and u satisfies (4.2) (in the obvious strong sense). A solution u is **maximal** if there do not exist a $T_1 > T$ and a solution u_1 on J_{T_1} extending u . In this case T is the maximal existence time of u .

Theorem 4.1. (i) *Problem (4.2) has for each (u^0, \bar{u}) satisfying (4.3) exactly one maximal solution u^* .*

(ii) *If T^* , the maximal existence time of u^* , is finite, then $u^* \notin \mathcal{H}_{q,p,\mathcal{B}}^{2,1}(Q_{T^*})$.*

Proof. Fix $T > 0$. Given $v \in \mathcal{H}(Q_T)$, put

$$A(\bar{u}, v)w := -\mathbf{a}(\bar{u}, v)\Delta w, \quad w \in H_{q,\mathcal{B}}^2.$$

We claim that $A(\bar{u}, v)$ has the property of maximal L_p regularity on $(0, \tau)$ for $0 < \tau \leq T$, meaning that the linear parabolic problem

$$(4.4) \quad \dot{w} + A(\bar{u}, v)w = g \quad \text{on } (0, \tau), \quad w(0) = 0$$

has for each $g \in L_p(J_\tau, L_q)$ exactly one solution $w \in \mathcal{H}(Q_\tau)$. To see this observe that, by (3.14),

$$a(\bar{u}, v)(t) \in C^p(\bar{\Omega}, (0, \infty))$$

for each fixed $t \in \bar{J}_T$. Thus a result of Prüss and Sohr [25] guarantees that the (time constant) operator

$$(w \mapsto A(\bar{u}, v)(t)w + \kappa w) \in \mathcal{L}(H_{q, \mathcal{B}}^2, L_q)$$

possesses for each $\kappa > 0$ and each $t \in \bar{J}_T$ bounded imaginary powers with a power angle less than $\pi/2$. Thus it follows from the Dore-Venni theorem (cf. [4, Theorems III.4.5.2 and III.4.10.8]) that $A(\bar{u}, v)(t)$ has for each fixed $t \in J_T$ the property of maximal L_p regularity. (Also see the much more general result [13, Theorem 8.2].) Now assertion (4.4) is a consequence of [5, Theorem 7.1].

Note that (3.12) implies that

$$A(\bar{u}, \cdot) \in \mathcal{C}^{1-}(\mathcal{H}(Q_T), L_\infty(J_T, \mathcal{L}(H_{q, \mathcal{B}}^2, L_q))).$$

Set

$$F(\bar{u}, v) := F_0(\bar{u}, v) + f(\cdot, v, \nabla v) + f_0, \quad v \in \mathcal{H}(Q_T).$$

From (3.4), (3.13), and (4.1) we easily infer that

$$F(\bar{u}, \cdot) - f_0 \in \mathcal{C}^{1-}(\mathcal{H}(Q_T), L_r(J_T, L_q)),$$

where $r > p$, due to (3.7) and $s > 1$. (We can assume that $s \leq p'$ since $T < \infty$.)

It is clear that problem (4.2) on J_T is equivalent to

$$(4.5) \quad \dot{u} + A(\bar{u}, u)u = F(\bar{u}, u) + f_0 \quad \text{on } (0, T), \quad u(0) = u^0.$$

It is also clear that $A(\bar{u}, \cdot)$ and $F(\bar{u}, \cdot)$ are Volterra maps in the sense that

$$(A(\bar{u}, v), F(\bar{u}, v)) |_{J_\tau} = (A(\bar{u}, v |_{J_\tau}), F(\bar{u}, v |_{J_\tau}))$$

for $0 < \tau < T$. Now the assertions of the theorem follow by applying [6, Theorem 2.1] to (4.5) for every $T > 0$. \square

Remark 4.2. In [6, (1.2)] there has to be added the hypothesis that $A(v)|_I$ has for every $v \in \mathcal{H}_p^1(J)$ and every perfect subinterval I of J the property of maximal L_p regularity. This assumption is needed in the proof of [5, Lemma 4.1] which, in turn, is used in the proof of [6, Theorem 2.1]. In [5, Lemma 4.1] it has only been shown that restrictions and translations of $\partial + A$ have bounded right inverses. The importance of that lemma lies in the uniform bounds established there.

Our next theorem shows that u^* depends continuously on all data. To make this precise we introduce the parameter space

$$\begin{aligned} \Xi := L_1 \cap L_s(J_S, \mathcal{L}(\mathbb{R}^m, \mathbb{R}^k)) &\times C^{2-}(\mathbb{R}^n, \mathbb{R}^m) \times C^{2-}(\bar{\Omega} \times \mathbb{R} \times \mathbb{R}^k) \\ &\times C^{1-}(\bar{\Omega} \times \mathbb{R} \times \mathbb{R}^n) \times L_p(\mathbb{R}^+, L_q) \times B_{q,p,\mathcal{B}}^{2-2/p} \times \mathcal{H}^-, \end{aligned}$$

endowed with its obvious Fréchet topology. Denoting by $\xi := (\omega, \alpha, a, f, f_0, u^0, \bar{u})$ its general point, we set

$$\Xi_0 := \{ \xi \in \Xi ; a(x, \xi, \eta) > 0 \text{ for } (x, \xi, \eta) \in \bar{\Omega} \times \mathbb{R} \times \mathbb{R}^k \}.$$



Note that Ξ_0 is open in Ξ . It follows from Theorem 4.1 that, given any $\xi \in \Xi_0$, problem (4.2) possesses a unique maximal solution. We denote it by $u(\xi)$ and write $T(\xi)$ for its maximal existence time.

Theorem 4.3. *Suppose that $\xi \in \Xi_0$ and fix $T \in (0, T(\xi))$. Then, given any sequence (ξ_j) , converging in Ξ_0 towards ξ , there exists $j_0 \in \mathbb{N}$ such that $T(\xi_j) > T$ for $j \geq j_0$ and $u(\xi_j) \rightarrow u(\xi)$ in $\mathcal{H}_{q,p,B}^{2,1}(Q_T)$.*

Proof. Using the continuity results (3.12) and (3.13) it is not difficult to see that the assertion follows from [6, Theorem 3.1] applied to (4.5). \square

5. PERONA-MALIK TYPE EQUATIONS

First we show that the theorems of the preceding section imply the validity of Theorem 1.1.

Proof of Theorem 1.1. (i) and (ii): Set $k := m := 1$, $\omega := |\theta|$, and $\alpha(y) := |y|^2$ for $y \in \mathbb{R}^n$, and denote by $\tilde{g} \in C^{2-}(\mathbb{R}, (0, \infty))$ a fixed extension of g . Also put $a(x, \xi, \eta) := \tilde{g}(\eta)$ for $(x, \xi, \eta) \in \bar{\Omega} \times \mathbb{R} \times \mathbb{R}$, and $(f, f_0) := (0, 0)$. Then (4.1) is satisfied and (4.2), with $\Gamma := \Gamma_1$, reduces to (1.17). Setting $\bar{u}(t) := u^0$ for $-S \leq t \leq 0$, it is obvious that $\bar{u} \in \mathcal{H}^-$. Hence (i) and (ii) follow from Theorem 4.1.

(iii) Since $\text{supp}(\theta) \subset [\sigma, S]$ for some $\sigma \in (0, S)$,

$$(5.1) \quad \omega * |\nabla u|^2(t) = \int_{t-S}^{t-\sigma} \omega(t-s) |\nabla u(s)|^2 ds, \quad t \geq 0.$$

Thus $\omega * |\nabla u|^2(t)$ depends on the values of $\nabla u(s)$ for $s \in [t-S, t-\sigma]$ only.

Suppose that $\xi \geq 0$. If $\xi = 0$, then set $u_1 := u^0$. Otherwise, suppose that $u_1 \in \mathcal{H}(Q_\xi)$ is a solution of (1.17) on J_ξ . Set $\Sigma_T := \Gamma \times (0, T)$ for $T > 0$ and

$$\bar{u}_1(t) := (\bar{u} \oplus u_1)(t + \xi), \quad -S_1 := -(S + \xi) \leq t \leq 0.$$

Consider

$$(5.2) \quad \begin{cases} \partial_t v - \nabla \cdot (g(\omega * |\nabla \bar{u}_1|^2) \nabla v) = 0 & \text{on } Q_\sigma, \\ \partial_\nu v = 0 & \text{on } \Sigma_\sigma, \\ v(\cdot, 0) = u_1(\xi) & \text{on } \Omega. \end{cases}$$

By (5.1) this problem is well defined on J_σ . Since $\bar{u}_1 \in \mathcal{H}(\Omega \times (-S_1, 0))$, it follows from (3.12) and (3.14) that the first equation of (5.2) can be written as

$$\partial_t v - a \Delta v + \vec{b} \cdot \nabla v = 0,$$

where $a \in C(\bar{J}_\sigma, C^\rho(\bar{\Omega}))$ with $a(x, t) > 0$ for $(x, t) \in \bar{Q}_\sigma$ and

$$(5.3) \quad \vec{b} \in L_r(J_\sigma, L_q(\Omega, \mathbb{R}^n)).$$

Set $A(t)v := -a(t)\Delta v$ for $v \in H_{q, \partial_\nu}^2$. Then we know from the proof of Theorem 4.1 that $A(t) \in \mathcal{L}(H_{q, \partial_\nu}^2, L_q)$ has for each $t \in \bar{J}_\sigma$ maximal L_p regularity, and $A \in C(\bar{J}_\sigma, \mathcal{L}(H_{q, \partial_\nu}^2, L_q))$. Put

$$B(t)v := \vec{b}(t) \cdot \nabla v, \quad v \in H_{q, \partial_\nu}^s,$$

where $1 + n/q < s < 2$. Note that such s exist since $1 + n/q < 2 - 2/p$ by (1.19). It is known (cf. [3, Theorem 5.2]) that $H_{q, \partial_\nu}^s = [L_q, H_{q, \partial_\nu}^2]_{s/2}$, where $[\cdot, \cdot]_\vartheta$ denotes the complex interpolation functor of exponent ϑ . Since

$$H_{q, \partial_\nu}^s \hookrightarrow H_q^s \hookrightarrow C^1(\bar{\Omega})$$



by a Sobolev embedding result (e.g., [27]), it follows from (5.3) that B belongs to $L_r \left(J_\sigma, \mathcal{L}(H_{q,\partial_\nu}^s, L_q) \right)$. Thus [5, Theorem 7.1] guarantees that $A + B$ has maximal L_p regularity. (Alternatively we could invoke [14, Theorem 2.1].) Observe that $u_1(\xi) \in B_{q,p,\partial_\nu}^{2-2/p}$ by (3.4). Thus it follows (e.g., [4, Theorem III.4.10.8]) that (5.2) possesses a unique solution $v_1 \in \mathcal{H}(J_\sigma)$. Set

$$u_2(t) := (\bar{u}_1 \oplus v_1)(t - \xi), \quad t \in J_{\xi+\sigma}.$$

Then $u_2 \in \mathcal{H}(\Omega_{\xi+\sigma})$ and it is a solution of (1.17), hence the unique one, on $Q_{\xi+\sigma}$. Thus by choosing successively $\xi = 0$, $\xi = \sigma$, $\xi = 2\sigma$, ... we see that (1.17) possesses a unique global solution.

(iv) follows from Theorem 4.3.

(v) Fix any $T \in (0, T^*)$. Since $p > 2$ and $q > 2$, it follows, in particular, that

$$u^* \in L_2(J_T, H^1) \cap H^1(J_T, H_{\partial_\nu}^{-1}) =: \mathcal{H}^{1,1}(Q_T),$$

where $H_{\partial_\nu}^{-1} := (H^1)'$ with respect to the duality pairing induced by the L_2 inner product, and that u^* is a weak solution on Q_T of the linear problem

$$(5.4) \quad \begin{cases} \partial_t u - \nabla \cdot (a^* \nabla u) = 0 & \text{on } Q_T, \\ a^* \partial_\nu u = 0 & \text{on } \Sigma_T, \\ u(\cdot, 0) = u^0 & \text{on } \Omega, \end{cases}$$

where $a^* := g(\omega * |\nabla u^*|^2) \in C(\bar{J}_T, C^\rho(\bar{\Omega}))$ with $a^*(x, t) > 0$ for $(x, t) \in \bar{Q}_T$. Now this assertion is an immediate consequence of the weak maximum principle.

(vi) The weak form of (5.4) implies that

$$(\langle u^*, \mathbf{1} \rangle)' = \left(\int_\Omega u^* \, dx \right)' = 0 \quad \text{in } \mathcal{D}'(0, T),$$



where $\mathbf{1}$ is the function being constantly equal to 1 on Ω , and $\mathcal{D}'(0, T)$ is the space of distributions on $(0, T)$. Since $\langle u^*, \mathbf{1} \rangle \in C(\overline{J}_T)$ by $u^* \in C(\overline{J}_T, L_2)$, it follows that $\langle u^*, \mathbf{1} \rangle(t) = \langle u^*, \mathbf{1} \rangle(0) = \langle u^0, \mathbf{1} \rangle$ for $0 \leq t \leq T$ and any $T \in (0, T^*)$.

(vii) Note that $u^* - \langle u^*, \mathbf{1} \rangle$ solves (5.4) with u^0 replaced by $u^0 - \langle u^0, \mathbf{1} \rangle$. Hence it suffices to prove that

$$(5.5) \quad \|u^*(s, t)\|_{L_s} \leq \|u^0\|_{L_s}, \quad 0 \leq t \leq T, \quad 2 \leq s \leq \infty,$$

where $T \in (0, T^*)$ is arbitrarily fixed and

$$u^0 \in B_{q,p,\delta_\nu}^{2-2/p} \hookrightarrow C(\overline{\Omega}) \hookrightarrow L_2$$

satisfies $\langle u^0, \mathbf{1} \rangle = 0$. From the weak formulation of (5.4) it follows that

$$(\|u^*\|_{L_2}^2)^\cdot \leq (\|u^*\|_{L_2}^2)^\cdot + 2\langle a^* \nabla u^*, \nabla u^* \rangle = 0 \quad \text{in } \mathcal{D}'(0, T).$$

This implies (5.5) for $s = 2$. Assertion (5.5) for $s = \infty$ is a consequence of (v). Now the assertion follows from the Riesz-Thorin interpolation theorem (e.g., [27]). \square

Proof of Remark 1.2(c). We can again assume that u^0 has mean value zero. For each $T \in (0, T^*)$ there exists $\beta > 0$ such that $g(\omega * |\nabla u^*(t)|^2) \geq \beta$ for $t \in J_T$. Thus the weak form of (5.4) implies

$$\begin{aligned} (\|u^*\|_{L_2}^2)^\cdot + \alpha \|u^*\|_{L_2}^2 &\leq (\|u^*\|_{L_2}^2)^\cdot + \beta \|\nabla u^*\|_{L_2}^2 \\ &\leq (\|u^*\|_{L_2}^2)^\cdot + (a^* \nabla u^*, \nabla u^*) = 0 \end{aligned}$$

in $\mathcal{D}'(0, T)$, where the existence of $\alpha = \alpha(T, \beta)$ is a consequence of Poincaré's inequality. Now the assertion follows. \square

Remarks 5.1. (a) Theorem 1.1 remains true if we modify (1.17) by replacing $\theta * |\nabla u|^2$ by $|\theta * \nabla u|^2$, or, more generally, by $|\boldsymbol{\theta} * \nabla u|^2$, where $\boldsymbol{\theta}$ is a diagonal matrix with diagonal entries $\theta_j \in L_s(J_S)$.

Proof. It suffices to put $k := m := n$ as well as $\alpha(\eta) := \eta$ and $a(x, \xi, \eta) := g(|\eta|^2)$ for $(x, \xi) \in \overline{\Omega} \times \mathbb{R}$ and $\eta \in \mathbb{R}^n$. \square

(b) Assertion (iii) remains valid if the right-hand side of the first equation in (1.17) is replaced by $f(x, u, \nabla u)$, provided f is linearly bounded in u and ∇u .

Proof. In this case one has to solve, instead of (5.2), a semilinear equation with a linearly bounded right-hand side. It is well known that such equations possess global solutions. \square

(c) Suppose that $v \in \mathcal{H}(Q_T)$. Then, given $u^0 \in B_{q,p,B}^{2-2/p}$, the linearized Perona-Malik problem

$$\begin{aligned} \partial_t u - \nabla \cdot (g(|\nabla v|^2) \nabla u) &= 0 && \text{on } Q_T, \\ \partial_\nu u &= 0 && \text{on } \Sigma_T, \\ u(\cdot, 0) &= u^0 && \text{on } \Omega \end{aligned}$$

possesses a unique solution $u(v) \in \mathcal{H}(Q_T)$. However, we have not succeeded in establishing a fixed point of the map $v \mapsto u(v)$ (for an appropriate $T > 0$) which would guarantee the existence of an $\mathcal{H}(Q_T)$ solution of (1.1). Anyhow, this observation indicates that (1.1) is ‘on the borderline to parabolic equations’ and explains to some extent why arbitrarily small time-delay perturbations of the Perona-Malik equation are well posed.

Proof. Set $a := g(|\nabla v|^2)$ and $\vec{b} := -2g'(|\nabla v|^2)D^2v\nabla v$ so that

$$-\nabla \cdot (g(|\nabla v|^2) \nabla u) = -a\Delta u + \vec{b} \cdot \nabla u$$

for $u \in \mathcal{H}(Q_T)$ It follows from (3.4) that $a \in C(\bar{J}, C(\bar{\Omega}))$ with $a(x, t) > 0$ for $(x, t) \in \bar{Q}_T$ and $\vec{b} \in L_p(J_T, L_q(\Omega, \mathbb{R}^n))$. Hence the assertion is implied by [14, Theorem 2.1], for example. \square

6. MODIFICATIONS

As discussed in the introduction, there are several possible modifications of the original Perona-Malik equation. For simplicity, we restrict ourselves to one such class. For this we suppose that

$$(6.1) \quad \left\{ \begin{array}{l} (1.19) \text{ is satisfied;} \\ g \in C^{2-}(\mathbb{R}^+, (0, \infty)); \\ h \in C^{2-}(\bar{\Omega} \times \mathbb{R}^+, (0, \infty)); \\ f \in C^{1-}(\Omega \times \mathbb{R} \times \mathbb{R}^n); \\ \theta \in L_s(J_S, \mathbb{R}^+) \text{ for some } s > 1 \text{ and } S > 0; \\ u^0 \in H_{q, \partial\nu}^2. \end{array} \right.$$

Then we consider the problem

$$(6.2) \quad \left\{ \begin{array}{ll} \partial_t u - \nabla \cdot (g(\theta * |\nabla u|^2) h(\cdot, u) \nabla u) = f(x, u, \nabla u) & \text{on } \Omega \times (0, \infty), \\ \partial_\nu u = 0 & \text{on } \Gamma \times (0, \infty), \\ u(\cdot, 0) = u^0 & \text{on } \Omega \times (-S, 0]. \end{array} \right.$$

In this model, besides of the edge enhancing function g , there is also a mechanism, namely the function h , which can prevent certain details of the image from being destroyed by diffusion. In fact, diffusion is slowed down at those points x in whose neighborhood $h(\cdot, u(\cdot))$ is small, even if $g(\theta * |\nabla u|^2)$ is large, that is, if $(\theta * |\nabla u|^2)^{1/2}$ is below the threshold value of the

original Perona-Malik model. Of course, in contrast to (1.1), in this case a priori information on the (correct) image is needed in order to choose the control function h appropriately.

Such a model has been proposed and studied by Kačur and Mikula [15], [16]. These authors consider the degenerate case also where h is allowed to vanish at some places. However, in contrast to our model (6.2), space regularization of CLMC type is employed in those papers.

Furthermore, the function f can be used to force the solution of (6.2) to stay close to the initial image u^0 . This is the case, for example, if

$$f(x, \xi, \eta) = \varphi(\xi - u^0(x)), \quad (x, \xi, \eta) \in \bar{\Omega} \times \mathbb{R} \times \mathbb{R}^n,$$

with a decreasing function φ . Such right-hand sides have been used by Nordström [22] (with $f(x, \xi, \eta) = u^0(x) - \xi$), Kačur and Mikula [15] (with

$$f(x, \xi, \eta) = \varphi(\beta(x, \xi) - \beta(x, u^0(x))),$$

where $\beta(x, \cdot)$ is increasing), and others (cf. [7]). Note, however, that in all those papers space convolution ∇u_σ is used instead of time convolution $\theta * |\nabla u|^2$.

Theorem 6.1. *Let assumptions (6.1) be satisfied. Then assertions (i) and (ii) of Theorem 1.1 hold for (6.2) also. The solution depends continuously on u^0 , θ , g , h , and f , in a sense analogous to assertion (iv) of Theorem 1.1.*

Proof. Set $k = m = 1$, $\omega := |\theta|$, $\alpha(y) := |y|^2$ for $y \in \mathbb{R}^n$, and

$$a(x, \xi, \eta) := \tilde{g}(\eta)h(x, \xi), \quad (x, \xi, \eta) \in \bar{\Omega} \times \mathbb{R} \times \mathbb{R}^n.$$

Then the assertions follow from Theorems 4.1 and 4.3. □



This theorem can be applied, in particular, to guarantee the well posedness of the Chen-Bose model (1.13) with ∇u_σ being replaced by the local term ∇u and the second order degenerate operator by the time regularized Perona-Malik operator $\nabla \cdot (g(\theta * |\nabla u|^2) \nabla u)$.

Acknowledgement. I am grateful to Jens Vogelgesang, Universität Bonn, for carrying out all numerical computations and providing the files for the figures of this paper.

1. Alvarez L., Guichard F., Lions P.-L., and Morel J.-M., *Axioms and fundamental equations of image processing*. Arch. Rational Mech. Anal. **123**(3) (1993), 199–257.
2. Alvarez L., Lions P.-L., and Morel J.-M. *Image selective smoothing and edge detection by nonlinear diffusion. II*. SIAM J. Numer. Anal. **29**(3) (1992), 845–866.
3. Amann H., *Nonhomogeneous linear and quasilinear elliptic and parabolic boundary value problems*. In Function spaces, differential operators and nonlinear analysis (Friedrichroda, 1992) volume 133 of *Teubner-Texte Math.*, pages 9–126. Teubner, Stuttgart, 1993.
4. ———, *Linear and Quasilinear Parabolic Problems, Volume I: Abstract Linear Theory*. Birkhäuser, Basel, 1995.
5. ———, *Maximal regularity for nonautonomous evolution equations*. Adv. Nonl. Studies, **4** (2004), 417–430.
6. ———, *Quasilinear parabolic problems via maximal regularity*. Advances in Diff. Equ., **10** (2005), 1081–1110.
7. Belahmidi A., *Équations aux dérivées partielles appliquées à la restauration et à l'aggrandissement des images*. PhD thesis, CEREMADE, Université Paris-Dauphine, Paris, 2003. <http://tel.ccsd.cnrs.fr>.
8. Belahmidi A. and Chambolle A., *Time-delay regularization of anisotropic diffusion and image processing*. M2AN Math. Model. Numer. Anal., **39**(2) (2005), 231–251.
9. Catté F., Lions P.-L., Morel J.-M. and Coll T.. *Image selective smoothing and edge detection by nonlinear diffusion*. SIAM J. Numer. Anal., **29**(1) (1992), 182–193.
10. Chen Y. and Bose P., *On the incorporation of time-delay regularization into curvature-based diffusion*. J. Math. Imaging Vision **14**(2) (2001), 149–164.

Home Page

Title Page

Contents



Page 51 of 52

Go Back

Full Screen

Close

Quit

11. Cottet G., El Ayyadi M., A Volterra type model for image processing. *IEEE Trans. Image Processing*, **7** (1998), 292–303.
12. Cottet G.-H. and Germain L., Image processing through reaction combined with nonlinear diffusion. *Math. Comp.*, **61**(204) (1993), 659–673.
13. Denk R., Hieber M. and Prüss J., \mathcal{R} -boundedness, Fourier multipliers and problems of elliptic and parabolic type. *Mem. Amer. Math. Soc.* **166**(788) (2003), viii+114.
14. ———, *Characterization of optimal L_p - L_q -estimates for parabolic boundary value problems by its data*, 2005. Preprint.
15. Kačur J. and Mikula K., *Solution of nonlinear diffusion appearing in image smoothing and edge detection*. *Appl. Numer. Math.* **17**(1) (1995), 47–59.
16. ———, *Slow and fast diffusion effects in image processing*. *Computation and Visualization in Science* **3** (2001), 185–195.
17. Kawohl B., *From Mumford-Shah to Perona-Malik in image processing*, *Math. Methods Appl. Sci.*, **27**(15) (2004), 1803–1814.
18. Kawohl B. and Kutev N., *Maximum and comparison principle for one-dimensional anisotropic diffusion*. *Math. Ann.* **311**(1) (1998), 107–123.
19. Kichenassamy S., *The Perona-Malik paradox*. *SIAM J. Appl. Math.* **57**(5) (1997), 1328–1342.
20. Mikula K. and Ramarosy N., *Semi-implicit finite volume scheme for solving nonlinear diffusion equations in image processing*. *Numer. Math.* **89**(3) (2001), 561–590.
21. Nitzberg M. and Shiotu T., *Nonlinear image filtering with edge and corner enhancement*. *IEEE Trans. Pattern Anal. and Machine Intelligence* **14** (1992), 826–833.
22. Nordström N., *Biased anisotropic diffusion – a unified regularization and diffusion approach to edge detection*. *Image Vision Compt.* **8** (1990), 318–327.
23. Perona P. and Malik J., *Scale-space and edge detection using anisotropic diffusion*. *IEEE Trans. Pattern Anal. Machine Intelligence* **12** (1990), 629–639.
24. Preusser T. and Rumpf M., *A level set method for anisotropic geometric diffusion in 3D image processing*. *SIAM J. Appl. Math.* **62**(5) (2002), 1772–1793 (electronic).
25. Prüss J. and Sohr H., *Imaginary powers of elliptic second order differential operators in L^p -spaces*. *Hiroshima Math. J.* **23** (1993), 161–192.
26. Sarti A., Mikula K., Sgallari F. and Lamberti C., *Evolutionary partial differential equations for biomedical image processing*. *J. for Biomedical Informatics* **35** (2002), 77–91.

[Home Page](#)

[Title Page](#)

[Contents](#)



Page 52 of 52

[Go Back](#)

[Full Screen](#)

[Close](#)

[Quit](#)

27. Triebel H., *Interpolation Theory, Function Spaces, Differential Operators*. North Holland, Amsterdam, 1978.
28. Weickert J., *Anisotropic diffusion in image processing*. European Consortium for Mathematics in Industry. B. G. Teubner, Stuttgart, 1998.

H. Amann, Institut für Mathematik, Universität Zürich, Winterthurerstr. 190, CH-8057 Zürich, Switzerland,
e-mail: herbert.amann@math.unizh.ch